Available online at www.sciencedirect.com
ScienceDirect
Electrochimica Acta 52 (2007) 4649–4653
ELECTROCHIMICA Acta
www.elsevier.com/locate/electacta

Oxygen reduction and diffusion in electroactive nanostructured membranes (ENM) using a layer-by-layer dendrimer-gold nanoparticle approach

Frank N. Crespilho [a,c], Francisco C. Nart [a,✠], Osvaldo N. Oliveira Jr. [b], Christopher M.A. Brett [c,*]

[a] *Instituto de Química de São Carlos, Universidade de São Paulo, 13560-970 São Carlos-SP, Brazil*
[b] *Instituto de Física de São Carlos, Universidade de São Paulo, 13560-970 São Carlos-SP, Brazil*
[c] *Departamento de Química, Universidade de Coimbra, 3004-535 Coimbra, Portugal*

Received 10 November 2006; received in revised form 4 January 2007; accepted 5 January 2007
Available online 2 February 2007

Dedicated to Prof. Francisco Nart, who died during the preparation of this paper.

Abstract

The fabrication of an electroactive nanostructured membrane (ENM) for oxygen reduction, made of layer-by-layer (LbL) films comprising Au nanoparticle-containing amine-terminated G4 PAMAM dendrimer alternated with poly(vinylsulfonic acid) (PVS) layers is reported. Electrochemical impedance spectroscopy and cyclic voltammetry show that electrodes with PVS/PAMAM-Au multiple bilayers are efficient for oxygen reduction and diffusion. A linear increase of oxygen reduction current occurs for up to 3 bilayers, with no further significant increase occurring for more than 3 bilayers. The 3-bilayer PVS/PAMAM-Au electrode, as an Au-ENM, is an attractive new system with potential for building diverse electrocatalytic devices with high molecular control.

Keywords: Gold nanoparticle electrodes; Electroactive nanostructured membranes; PAMAM dendrimers; Oxygen reduction; Layer-by-layer

1. Introduction

The use of dendrimers in layer-by-layer (LbL) films has proven promising for applications in catalysis [1] and biosensors [2–4], including cases in which intricate multilayer structures are built [5]. This versatility arises from the unique properties of dendrimers, namely specific terminal groups and a nearly perfect hyperbranched topology radiating from a central core. Poly(amido amide) (PAMAM) dendrimers, for instance, can be used in electroactive nanostructured membranes (ENM), since metallic nanoparticles are formed by reduction of the corresponding ions inside the dendrimer molecules. Various strategies of synthesis and application of dendrimer-nanoparticles have been proposed by Crook and co-workers [6–8]. Recently, we have introduced the concept of ENM for electrochemical applications, in particular electrocatalytic membranes for fuel cell electrodes [1] and sensors [9]. Using PAMAM molecules and the LbL approach, different kinds of ENM were prepared, viz. PAMAM-Pt [1], PAMAM-Au-enzyme [9] and PAMAM-Au@Me core–shell system [2], where Me is a redox mediator immobilized around the metallic nanoparticle. The ENM is advantageous owing to its controlled porosity and electroactive area, high ionic permeability, molecularly-controlled structure and high electrochemical stability [1,5,9].

In order to examine the capability for oxygen diffusion through ENMs, in this work we investigate this at ENMs consisting of nanoparticle-containing amine-terminated G4 PAMAM dendrimer and poly(vinylsulfonic acid) (PVS) multilayers fabricated using the LbL technique. Nanosized Au nanoparticles were grown inside PAMAM molecules using formic acid as the reducing agent. This membrane was used to probe the electrocatalytic properties of oxygen reduction and diffusion. The electroreduction of oxygen is important for electrochemical energy storage, industrial processes and biosensors. Also, using Au nanoparticles for oxygen electroreduction may bring a new approach to electrochemical surface science, since the nanoparticles exhibit properties differing from those of bulk gold electrodes [10].

* Corresponding author.
E-mail address: brett@ci.uc.pt (C.M.A. Brett).
✠ Deceased.

0013-4686/$ – see front matter © 2007 Elsevier Ltd. All rights reserved.
doi:10.1016/j.electacta.2007.01.048

Furthermore, this study can open the way to further studies involving gas permeability across LbL membranes.

2. Experimental

2.1. Synthesis of the gold nanoparticles

PAMAM-Au nanohybrids were prepared as follows: 2 mL of $KAuCl_4$ solution (1 mmol L^{-1}) were added to 2 mL of PAMAM (0.07 mmol L^{-1}) and 2 mL of formic acid (1 mmol L^{-1}). This pale yellow solution was vigorously stirred for 2 min. When the zerovalent Au complex was formed the colour immediately changed from yellow to red. This reaction occurred over a 4-h time period and the nanoparticle growth kinetics was followed by UV–vis spectroscopy (Hitachi U-2001 Spectrophotometer; San Jose, CA, USA). The morphology and particle size distribution were characterized using a 200 kV transmission electron microscope (TEM, Model CM200; Philips, Eindhoven, the Netherlands). The particle size distribution was estimated by measuring the diameter of at least 200 particles in TEM images.

2.2. PVS/PAMAM-Au LbL films

PVS/PAMAM-Au LbL multilayers were assembled onto ITO-coated glass. The concentration of the dipping solutions was set at 0.07 mmol L^{-1} and 0.5 g L^{-1} for PAMAM-Au and PVS, respectively. The sequential deposition of multilayers was carried out by immersing the substrates alternately into the PAMAM-Au and PVS solutions for 5 min (Scheme 1). After deposition of each layer, the substrate/film system was rinsed with water (Milipore Milli-Q nanopure water, resistivity > 18 MΩ cm). The growth of the multilayers was monitored by cyclic voltammetry.

2.3. Electrochemical measurements

Cyclic voltammograms were obtained of films containing different numbers of PVS/PAMAM-Au (Au-ENM) layers deposited onto ITO-covered substrates using a CV-50 W Voltammetric Analyzer from Bioanalytical Systems, West Lafayette, IN, controlled by BAS CV-2.1 software. The electrochemical cell was a three-electrode system. An Ag/AgCl (sat. KCl) electrode was used as reference, Pt wire as counter electrode and bare ITO or ITO covered with a PVS/PAMAM-Au multilayer film as working electrode. All electrodes were inserted into the electrochemical cell containing a 0.1 mol L^{-1} H_2SO_4 solution and the voltammogram was immediately recorded. The voltammograms were recorded at 20 °C at different scan rates.

Electrochemical impedance measurements were carried out using a Solartron 1250 frequency response analyzer, coupled to a Solartron 1286 electrochemical interface controlled by Zplot software. A sinusoidal voltage perturbation of amplitude 10 mV rms was applied in the frequency range between 65 kHz and 0.1 Hz with a 10 frequency steps per decade. The values of resistance and capacitance were obtained in three independent experiments with each of three different working electrodes and the data errors were calculated from Student's *t*-distribution, with 9 degrees of freedom and 99.5% confidence level. Values of resistance and capacitance were estimated from fitting of the spectra using ZPlot software.

2.4. Oxygen reduction experiments

Two kinds of electrodes were used to compare the catalytic properties of Au-ENM: bare ITO and ITO modified with PVS/PAMAM-Au-ENM. First, an ITO electrode was modified with a different number of bilayers of PVS/PAMAM-Au and the results were compared with a bare ITO electrode using linear scan voltammetry. Impedance spectroscopy was used to estimate the charge transport with the bare ITO and ITO-PVS/PAMAM-Au multilayer modified electrodes, in which oxygen reduction can occur on the surface of the Au nanoparticles. In order to verify the influence of Au nanoparticles on the oxygen reduction, experiments were also carried out with PVS/PAMAM (without Au nanoparticles) modified electrodes.

All experiments were performed in air-saturated 0.1 mol L^{-1} H_2SO_4 solution at 25 ± 1 °C.

3. Results and discussion

The formation of PAMAM-Au nanoparticles in aqueous suspension was monitored via UV–vis spectroscopy (not shown), where the peak around 500 nm was associated with the plas-

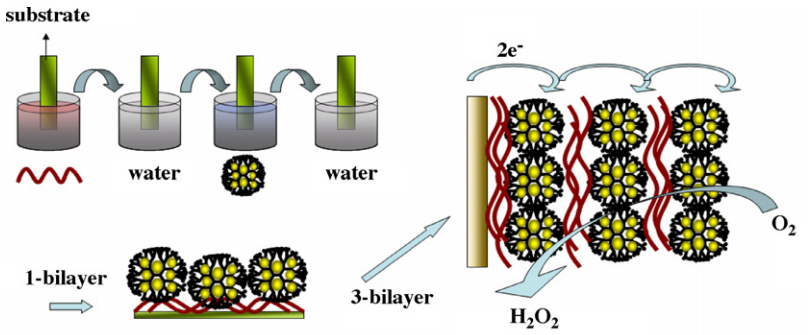

Scheme 1. Schematic fabrication of LbL films comprising PVS and PAMAM-Au. The sequential deposition of LbL multilayers was carried out by immersing the substrates alternately into PVS and PAMAM-Au solutions for 5 min per step. After deposition of 3 bilayers, an ITO-(PVS/PAMAM-Au)$_3$ electrode was prepared and oxygen reduction was carried out in air-saturated 0.1 mol L^{-1} H_2SO_4 solution.

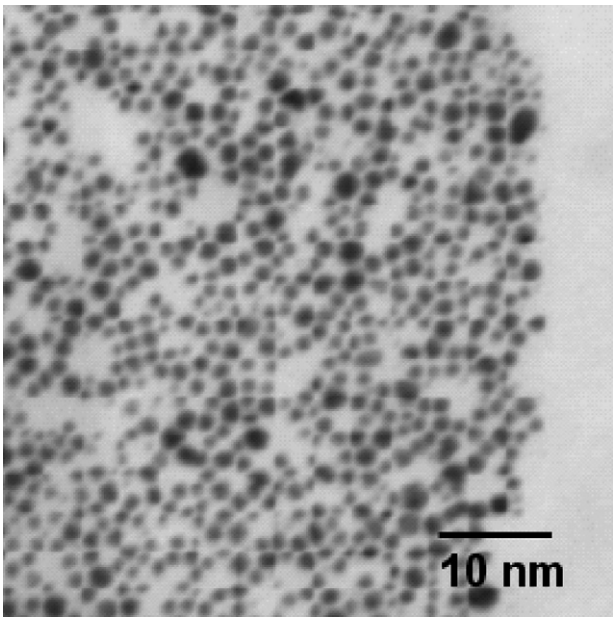

Fig. 1. Bright-field TEM image of Au nanoparticles.

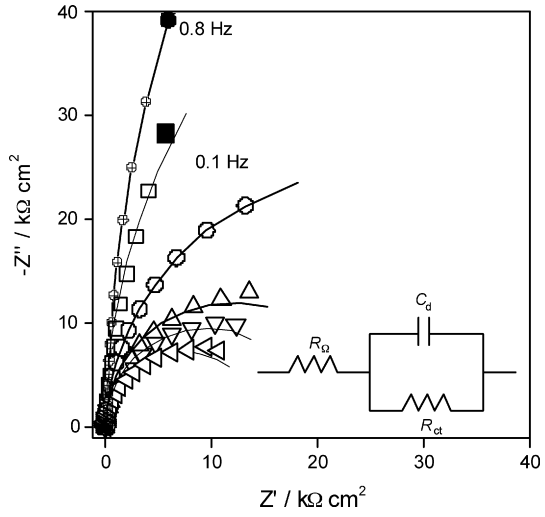

Fig. 2. Complex plane impedance spectra for ITO (⌖) and ITO-(PVS/PAMAM-Au)$_n$, with n = 1 (□), 2 (◯), 4 (△), 6 (▽) and 8 (◁) bilayers at an applied potential of −50 mV vs. Ag/AgCl. In the inset, the equivalent circuit used in the fitting (continuous line) for oxygen reduction on Au-ENM. Electrolyte: air-saturated 0.1 mol L^{-1} H_2SO_4 solution.

mon resonance [2,11]. Results obtained with TEM after 200 min reaction for a one-layer cast film on a copper grid showed well-organized Au particles, with a particle diameter of approximately 3 nm (as shown in Fig. 1). The same PAMAM-Au solution was used to produce cationic layers, which were alternated with PVS adsorption onto ITO substrates in a layer-by-layer fashion, thus leading to the structure Au-ENM shown in Scheme 1. The multilayer growth was monitored by cyclic voltammetry, where a linear increase of the anodic and cathodic peak currents from Au nanoparticles was observed, indicating that the same amount of material is adsorbed during each deposition step [1,2,5].

Electrochemical impedance spectroscopy was used to examine the influence of Au nanoparticles on oxygen reduction for the LbL films. Fig. 2 shows well-defined spectra in the complex plane for ITO-PVS/PAMAM-Au multilayers due to the oxygen reduction reaction at an applied potential of −50 mV versus Ag/AgCl. These impedance results were interpreted with a model of an electroactive membrane which considers the formation of electrocatalytic sites (gold nanoparticles) in the films during the LbL process. The electroactive membrane model is based on the organic membrane model [12–16], which consists in an organic film deposited on a conducting substrate. In our case, the organic film is represented by a multilayer containing gold nanoparticles. The membrane model can be applied by representing the electrochemical cell as a simple RC parallel combination [12], where the capacitance and resistance values of the film are both related with film thickness, i.e. the number of nanoparticles. This influences the total measured double layer charge, and thence the capacitance, as well as the rate of electrochemical reactions, represented by a charge transfer resistance. Since nanoparticles are available to react with the oxygen dissolved in the electrolyte solution, the resistance associated with this process depends inversely on the number of nanoparticles deposited. Thus, the membrane model of Au-ENM for oxygen reduction and its equivalent circuit can be represented as depicted in the inset of Fig. 2.

In this case, the faradaic process is associated with oxygen reduction. The charge-transfer resistance in the film should therefore by inversely proportional to the amount of available catalytic sites inside the film. The components of the equivalent electrical circuit are represented by the cell resistance, R_Ω, the charge-transfer resistance for oxygen reduction, R_{ct}, while C_d is the double-layer capacitance for n-bilayers. Thus, the total impedance can be expressed by Eq. (1):

$$Z(\omega) = R_\Omega + \frac{1}{i\omega C_d + (1/R_{ct})} \quad (1)$$

Owing to the high total impedance values recorded, the cell resistance $R_\Omega = 150\,\Omega$ can be ignored. Eq. (1) satisfies the criterion that if the film has an increasing concentration of electrocatalytic sites for oxygen reduction, the total impedance should be lower. Fig. 3 shows that R_{ct} decreases with an increasing number of bilayers in an exponential fashion. This dependence implies that oxygen reduction occurs at all the gold nanoparticle sites in the film up to 3 bilayers. With more than 3 bilayers, the sites in the innermost layers, which are further from the external electrolyte interface, are probably not accessible due to blocking by subsequent layers and/or oxygen does not diffuse through. There could also be some influence from hindered electrical communication from the ITO substrate to the outermost layers, as discussed in refs. [3,4].

When the film has a high charge transfer resistance, the capacitance should vary with film thickness, which was confirmed for an ITO-PVS/PAMAM multilayer without gold nanoparticles employed under the same conditions, as shown in Fig. 4. With the PVS/PAMAM bilayers there occurs a decrease in C_d and an increase in R_{ct}. Eq. (1) was applied, resulting in excellent agreement with the experimental results, as also shown in Fig. 4. The values of C_d using 1 and 10 bilayers of PVS/PAMAM are

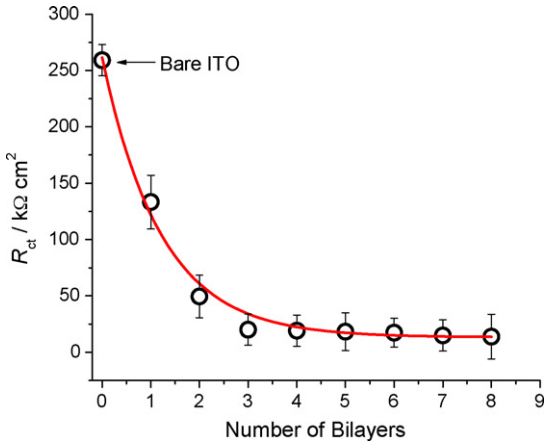

Fig. 3. Charge-transfer resistance (R_{ct}) for oxygen reduction vs. number of PVS/PAMAM-Au bilayers. R_c was obtained using three different electrodes and the data errors were calculated from nine spectra (three R_{ct} values per electrode).

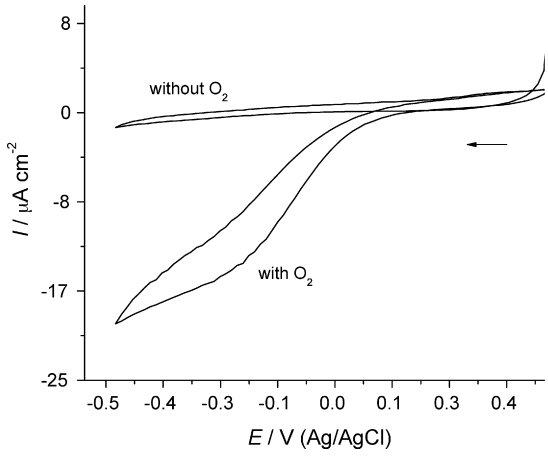

Fig. 5. Cyclic voltammetry of a 3-bilayer ITO-PVS/PAMAM-Au modified electrode in 0.1 mol L^{-1} H_2SO_4 solution with and without dissolved oxygen. Scan rate 10 mV s^{-1}.

4.56 ± 0.09 and 7.60 ± 0.03 μF, respectively, as expected for the increased film thickness.

Fig. 5 shows two voltammograms obtained using 3-bilayer ITO-(PVS/PAMAM-Au) electrodes in 0.1 mol L^{-1} H_2SO_4 solution in the presence and absence of dissolved oxygen. A well-defined voltammogram for oxygen reduction can be observed. The cathodic peak for oxygen reduction appears at −0.3 V and, as expected, by varying the scan rate, ν, the charge transfer is seen to be diffusion-limited up to 300 mV s^{-1} in the I versus $\nu^{1/2}$ plot (Fig. 6).

Since the voltammogram from the 3-bilayer ITO-PVS/PAMAM-Au modified electrode displayed a well-defined performance, with a lower capacitive and a higher faradaic current, it can be deduced that the presence of Au nanoparticles in this structure promotes a more efficient oxygen reduction than in their absence and that the membrane permits oxygen diffusion. The reduction current peak remains the same after repeated cycling of the applied potential, showing the structure to be highly stable. Therefore, there is no induced agglomeration of Au nanoparticles on the electrode surface [10], consistent with the previously observed fact that immobilized species in LbL membranes show a well-defined stability and that Au nanoparticles are strongly encapsulated inside the dendrimer molecules [1,2,6–9]. PAMAM dendrimer multilayers offer a high molecular control which can be effectively used as the conjugating units for the construction of spatially ordered nanostructures, such as thickness-controlled biosensing interfaces [3] and in enzyme electrodes [4,9].

Fig. 7 shows linear scan voltammograms at 10 mV s^{-1} scan rate for a bare ITO and a 3-bilayer ITO-PVS/PAMAM-Au electrode in 0.1 mol L^{-1} H_2SO_4 solution. The values of the currents were normalized by the exposed geometric area of the ITO-PVS/PAMAM-Au electrode. With the modified ITO electrode, oxygen reduction begins at around 0.0 V and the cathodic current increases gradually as the potential is swept negatively. For example, at −50 mV (the same potential used in electrochemical impedance experiments) the reduction current was -0.71 ± 0.03, -1.12 ± 0.03 and -1.73 ± 0.03 μA cm^{-2}

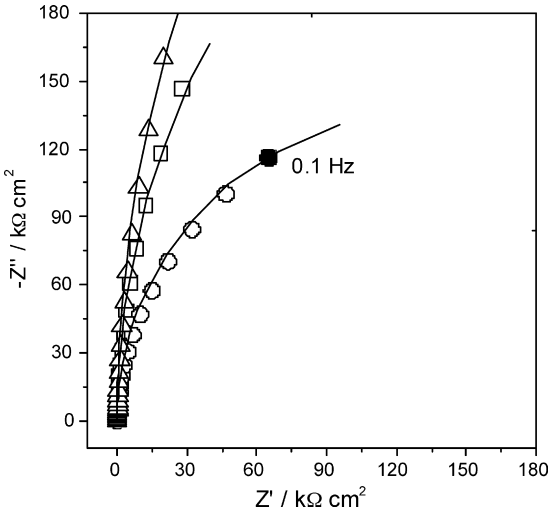

Fig. 4. Complex plane impedance spectra for ITO (◯), 1-bilayer PVS/PAMAM (□) and 10-bilayer (△) PVS/PAMAM at an applied potential of −50 mV vs. Ag/AgCl. The equivalent circuit used in the fitting (continuous line) for oxygen reduction is the same as in Fig. 1. Electrolyte: air-saturated 0.1 mol L^{-1} H_2SO_4 solution.

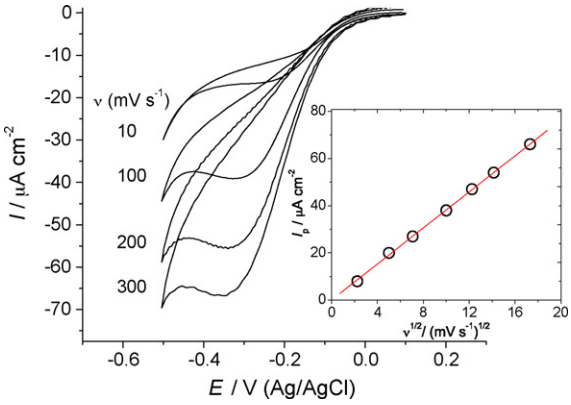

Fig. 6. Influence of scan rate (ν: 10, 100, 200 and 300 mV s^{-1}) on reduction peak current of a 3-bilayer ITO-PVS/PAMAM-Au modified electrode. Ten successive cycles with the same current values were obtained at each scan rate. In the inset, a plot of I_p vs. $\nu^{1/2}$. Electrolyte: air-saturated 0.1 mol L^{-1} H_2SO_4 solution.

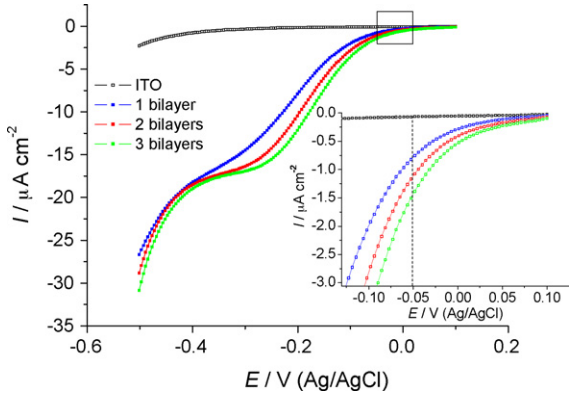

Fig. 7. Linear scan voltammograms at 10 mV s^{-1} for oxygen reduction using bare ITO and 1–3-bilayer ITO-PVS/PAMAM-Au modified electrodes. In the inset, magnified scan region around 0.00 V. Electrolyte: air-saturated 0.1 mol L^{-1} H_2SO_4 solution.

for 1–3 PVS/PAMAM-Au bilayers, respectively. This increase in oxygen reduction current with the number of bilayers agrees with the results from the impedance experiments, since the charge-transfer resistance decreases significantly up to 3 bilayers. Also, a faster increase in cathodic current associated with 3 bilayers, the ITO-$(PVS/PAMAM\text{-}Au)_3$ electrode, is easily identified, and reflects a faster electron transfer at the PAMAM-Au multilayer on the electrode. On the other hand, when a bare ITO electrode was used, no oxygen reduction current was observed. Evidence for the two-electron mechanism to hydrogen peroxide is due to the fact that hydrogen peroxide reduction occurs at a more negative potential [10]. The diffusion-limited current is reached between −0.33 and −0.46 V. Below −0.46 V, the reduction of electrogenerated hydrogen peroxide leads to a further increase in current at more negative values of potential.

4. Conclusions

Using a 1–3-bilayer PVS/PAMAM-Au electrodes, prepared by the LbL technique, oxygen reduction was successfully demonstrated by linear scanning of the potential, the oxygen reduction current increasing with the number of bilayers. Electrochemical impedance spectroscopy was also used to investigate the influence of Au nanoparticles on oxygen reduction, in electroactive nanostructured membranes. In comparison to a bare ITO electrode, the ITO-PVS/PAMAM-Au electrode displayed good performance for oxygen reduction, the Au nanoparticles showing catalytic activity for oxygen reduction and promoting charge-transfer across PVS/PAMAM-Au multilayers. From the electrochemical impedance data, a simple membrane model for ENM was proposed to explain how the charge transfer occurs. An important conclusion was that oxygen permeability occurs easily for up to 3 bilayers of PAMAM-Au, with little extra benefit being obtained from using thicker films with more than 3 bilayers.

Acknowledgements

Financial support from FAPESP, Capes (process number 1238/05-1), CNPq, IMMP/MCT (Brazil) and Fundação para a Ciência e Tecnologia (FCT) Portugal, ICEMS (Research Unit 103) is gratefully acknowledged.

References

[1] F.N. Crespilho, F. Huguenin, V. Zucolotto, P. Olivi, F.C. Nart, O.N. Oliveira Jr., Electrochem. Commun. 8 (2006) 348.
[2] F.N. Crespilho, V. Zucolotto, C.M.A. Brett, O.N. Oliveira Jr., F.C. Nart, J. Phys. Chem. B 110 (2006) 17478.
[3] H.C. Yoon, H.S. Kim, Anal. Chem. 72 (2000) 922.
[4] H.C. Yoon, M.Y. Hong, H.S. Kim, Anal. Chem. 72 (2000) 4420.
[5] F.N. Crespilho, V. Zucolotto, J.R. Siqueira Jr., C.J.L. Constantino, F.C. Nart, O.N. Oliveira Jr., Environ. Sci. Technol. 39 (2005) 5385.
[6] M.Q. Zhao, R.M. Crooks, Adv. Mater. 11 (1999) 217.
[7] M.Q. Zhao, R.M. Crooks, Chem. Mater. 11 (1999) 3379.
[8] H. Ye, R.M. Crooks, J. Am. Chem. Soc. 127 (2005) 4930.
[9] F.N. Crespilho, M.E. Ghica, M. Florescu, F.C. Nart, O.N. Oliveira Jr., C.M.A. Brett, Electrochem. Commun. 8 (2006) 1665.
[10] C.R. Raj, A.I. Abdelrahman, T. Ohsaka, Electrochem. Commun. 7 (2005) 888.
[11] F.N. Crespilho, T.F.C.C. Borges, V. Zucolotto, E.R. Leite, F.C. Nart, O.N. Oliveira Jr., J. Nanosci. Nanotechnol. 6 (2006) 2588.
[12] J.N. Murray, Prog. Org. Coat. 30 (1997) 225.
[13] N. Tang, W.J. van Oooij, G. Gorecki, Prog. Org. Coat. 30 (1997) 255.
[14] J.N. Murray, Prog. Org. Coat. 31 (1997) 275.
[15] F.N. Crespilho, V. Zucolotto, J.R. Siqueira Jr., A.J.F. Carvalho, F.C. Nart, O.N. Oliveira Jr., Int. J. Electrochem. Sci. 1 (2006) 151.
[16] F.N. Crespilho, V. Zucolotto, O.N. Oliveira Jr., F.C. Nart, Int. J. Electrochem. Sci. 1 (2006) 194.